Title

Targeted Multifunctional Lipid ECO Plasmid DNA Nanoparticles as Efficient Non-viral Gene Therapy for Lebers Congenital Amaurosis.

Authors

Sun, Da
Sahu, Bhubanananda
Gao, Songqi
et al.

Publication Date

2017-06-16

DOI

10.1016/j.omtn.2017.02.005

Peer reviewed

Molecular Therapy
Nucleic Acids
Original Article

Targeted Multifunctional Lipid ECO Plasmid DNA Nanoparticles as Efficient Non-viral Gene Therapy for Leber's Congenital Amaurosis

Da Sun,[1] Bhubanananda Sahu,[2] Songqi Gao,[3] Rebecca M. Schur,[1] Amita M. Vaidya,[1] Akiko Maeda,[2] Krzysztof Palczewski,[3] and Zheng-Rong Lu[1]

[1]Case Center for Biomolecular Engineering and Department of Biomedical Engineering, School of Engineering, Case Western Reserve University, Cleveland, OH 44106, USA; [2]Department of Ophthalmology and Visual Sciences, School of Medicine, Case Western Reserve University, Cleveland, OH 44106, USA; [3]Department of Pharmacology and Cleveland Center for Membrane and Structural Biology, School of Medicine, Case Western Reserve University, Cleveland, OH 44140, USA

Development of a gene delivery system with high efficiency and a good safety profile is essential for successful gene therapy. Here we developed a targeted non-viral delivery system using a multifunctional lipid ECO for treating Leber's congenital amaurosis type 2 (LCA2) and tested this in a mouse model. ECO formed stable nanoparticles with plasmid DNA (pDNA) at a low amine to phosphate (N/P) ratio and mediated high gene transfection efficiency in ARPE-19 cells because of their intrinsic properties of pH-sensitive amphiphilic endosomal escape and reductive cytosolic release (PERC). All-*trans*-retinylamine, which binds to interphotoreceptor retinoid-binding protein (IRBP), was incorporated into the nanoparticles via a polyethylene glycol (PEG) spacer for targeted delivery of pDNA into the retinal pigmented epithelium. The targeted ECO/pDNA nanoparticles provided high GFP expression in the RPE of 1-month-old *Rpe65*$^{-/-}$ mice after subretinal injection. Such mice also exhibited a significant increase in electroretinographic activity, and this therapeutic effect continued for at least 120 days. A safety study in wild-type BALB/c mice indicated no irreversible retinal damage following subretinal injection of these targeted nanoparticles. All-*trans*-retinylamine-modified ECO/pDNA nanoparticles provide a promising non-viral platform for safe and effective treatment of RPE-specific monogenic eye diseases such as LCA2.

INTRODUCTION

Leber's congenital amaurosis (LCA) is a genetic disease causing retinal degeneration with severe vision loss at an early age that affects 1 in 80,000 subjects.[1–3] One molecular form of this disease, LCA type 2 (LCA2), is caused by mutations in the *RPE65* gene that encodes the RPE65 protein (retinal pigment epithelium-specific protein 65-kDa) predominantly expressed in the retinal pigmented epithelium (RPE). RPE65, a key enzyme in retinoid metabolism, catalyzes the hydrolysis and isomerization of all-*trans*-retinyl esters to 11-*cis*-retinal. *RPE65* deficiency results in the accumulation of all-*trans*-retinyl esters and causes rod and cone photoreceptor dysfunction.[4–6]

Currently, there is no approved therapy for effectively treating LCA2. As a monogenic disease, LCA2 is a good candidate for gene therapy because the photoreceptor cells and the RPE do not show extensive pathological abnormalities in the early stages of this disease.[7] Recently, gene replacement therapy with adeno-associated viral vectors (AAVs) has demonstrated considerable therapeutic efficacy in improving vision in *RPE65*-deficient animal models and human patients.[8–13] Although clinical trials have validated the overall benefit of gene replacement therapy, their success is limited by several drawbacks associated with viral delivery systems. The possibility of an immune response induced by viral vectors greatly compromises the efficiency of gene transfection and can cause complications in patients.[14] Studies have shown that vector DNA is detectable in the optic nerve and brain following subretinal injections, which raises additional safety concerns.[15]

Non-viral gene delivery systems that employ cationic lipids, dendrimers, polycations, and polysaccharides have also been developed for gene delivery.[16–20] Non-viral systems generally exhibit advantages such as ease of production, good safety profiles, and unlimited cargo capacity. However, their clinical translation is still hindered by their low transfection efficiency and transient gene expression.[21] Novel designs of highly effective non-viral delivery systems are needed to overcome the limitations of existing non-viral delivery systems for gene therapy of inherited monogenic visual disorders to become effective and practical.

Recently, we designed a multifunctional lipid, (1-aminoethyl)iminobis [N-(oleicylcysteinyl-1-amino-ethyl)propionamide] (ECO), as a simple and smart gene delivery carrier based on its mechanism of pH-sensitive amphiphilic endosomal escape and reductive cytosolic release (PERC) of nucleic acids.[22–26] ECO contains a protonable

Received 12 November 2016; accepted 11 February 2017;
http://dx.doi.org/10.1016/j.omtn.2017.02.005.

Correspondence: Zheng-Rong Lu, Department of Biomedical Engineering, Case Western Reserve University, Wickenden 427, Mail Stop 7207, 10900 Euclid Avenue, Cleveland, OH 44106, USA.
E-mail: zxl125@case.edu

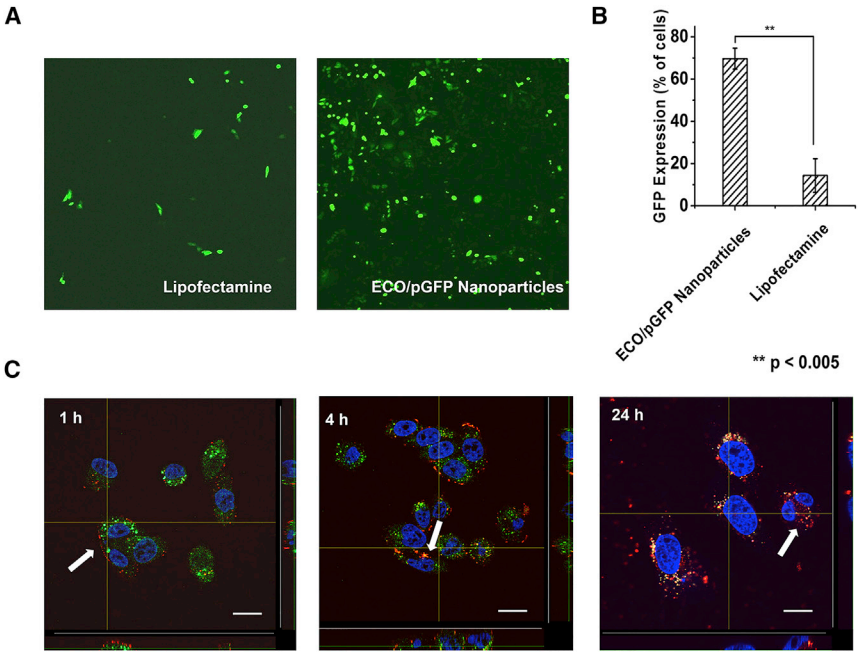

Figure 1. In Vitro Transfection of ARPE19 Cells with ECO/pDNA Nanoparticles

(A and B) Confocal microscopy images (A) and flow cytometry analysis (B) of ARPE-19 cells transfected with ECO/pGFP (N/P = 6) nanoparticles and Lipofectamine 2000/pGFP nanoparticles for 48 hr (**$p < 0.005$). Each bar represents the mean ± expression level of GFP (n = 3). (C) Confocal fluorescence microscopy images demonstrating intracellular trafficking of ECO/Cy3-pDNA nanoparticles in ARPE-19 cells. Cells were treated with LysoTracker Green (1:2,500 dilution) and Hoechst 33342 (1:10,000 dilution) and then transfected with ECO/Cy3-labeled nanoparticles at N/P = 6. After 1, 4, and 24 hr of transfection, cells were fixed and imaged. Green, endosomes; blue, nuclei; red, Cy3-labeled pDNA. Arrows denote the ECO/Cy3-pDNA nanoparticles and Cy3-pDNA. Scale bars, 20 μm.

ethylenediamine (E) head group, two cysteine (C) functional linkers, and two oleoyl (O) lipophilic tails. The thiol groups of the cysteine residues can form disulfide bonds to stabilize particle formulations and can also be chemically modified with targeting ligands. Following cellular uptake, cytosolic release of the gene cargo is facilitated by pH-sensitive amphiphilic endosomal membrane destabilization through protonation of the head group of ECO in the acidic endosomal-lysosomal compartment (pH = 5–6) and dissociation of the nanoparticles by reduction of the disulfide bonds in the cytoplasm. ECO has demonstrated excellent transfection efficiency for RNAi cancer therapies without additional helper lipids.[25] An ECO/dendrimer hybrid system has also successfully transfected retinal tissue with GFP.[26]

In this study, we designed and prepared all-*trans*-retinylamine modified ECO plasmid DNA (pDNA) nanoparticles with a polyethylene glycol (PEG) spacer to target interphotoreceptor retinoid-binding protein (IRBP) for enhanced gene delivery into the retina. All-*trans*-retinoids have a high binding affinity for retinoid binding proteins, which play important roles in visual transduction.[27] IRBP is a major protein in the interphotoreceptor matrix (IPM) that selectively transports 11-*cis*-retinal to photoreceptor outer segments and all-*trans*-retinol to the RPE.[28–33] Such a selective transport mechanism can increase the transfection efficiency directly into the RPE with the ECO/pDNA nanoparticles conjugated with all-*trans*-retinylamine. We first evaluated the in vitro transfection efficiency of ECO/pDNA nanoparticles in ARPE-19 cells, a human RPE cell line. The in vivo transfection efficiency of targeted ECO/pDNA nanoparticles to the RPE was then evaluated in wild-type BALB/c mice using GFP plasmids. Finally, the efficacy of gene therapy with the targeted nanoparticles was determined by electroretinography (ERG) in the *Rpe65*$^{-/-}$ mouse model of human LCA2.

RESULTS

In Vitro Transfection with ECO/pDNA Nanoparticles

To determine the transfection efficiency of ECO in vitro, human RPE cells (ARPE-19) were transfected with ECO/plasmid GFP (pGFP; amine to phosphate [N/P] ratio = 6/1) nanoparticles, and confocal microscopy was used to determine GFP expression 48 hr after transfection (Figure 1A). ECO/pGFP nanoparticles produced significant GFP expression, with 69.7% of cells expressing GFP, whereas the Lipofectamine control transfected only 14.4% of the cells, as determined by flow cytometry (Figure 1B). The high gene expression efficiency of ECO/pDNA nanoparticles correlated positively with their efficient intracellular uptake. Figure 1C shows the intracellular uptake of ECO/pDNA nanoparticles as imaged by 3D confocal microscopy 1, 4, and 24 hr post-transfection with Cy3-pDNA as the tracker. After 1 hr incubation, ECO/Cy3-pDNA nanoparticles (red) were aligned at the surface of the cell membrane because of electrostatic interactions of these positively charged nanoparticles with the negatively charged cell membrane. After 4 hr, the nanoparticles entered the cell and co-localized with late endosomes, indicated by their yellow color. After 24 hr, the nanoparticles escaped endosomal entrapment, as shown by the red fluorescence in the cytoplasm and the diminished overlap with endosomes. Efficient cytosolic pDNA delivery of ECO/pDNA nanoparticles resulted in high gene expression efficiency in RPE cells in vitro.

Preparation of Retinylamine-Targeted ECO/pDNA Nanoparticles

To target IRBP, an all-*trans*-retinoid structure was introduced onto the surface of ECO/pDNA nanoparticles via a PEG (3.4-kDa) spacer. All-*trans*-retinylamine (all-*trans*-retinylamine [Ret]-NH_2) was first reacted with the N-hydroxysuccinimide (NHS)-activated ester of NHS-PEG-malaimido (MAL) to yield Ret-PEG-MAL, which was characterized by MALDI-TOF mass spectroscopy (Figures 2A and 2B). To form targeted ECO/pDNA nanoparticles, Ret-PEG-MAL was first reacted with the 2.5 mol % ECO via Michael addition between the thiol and maleimide. The targeted nanoparticles were

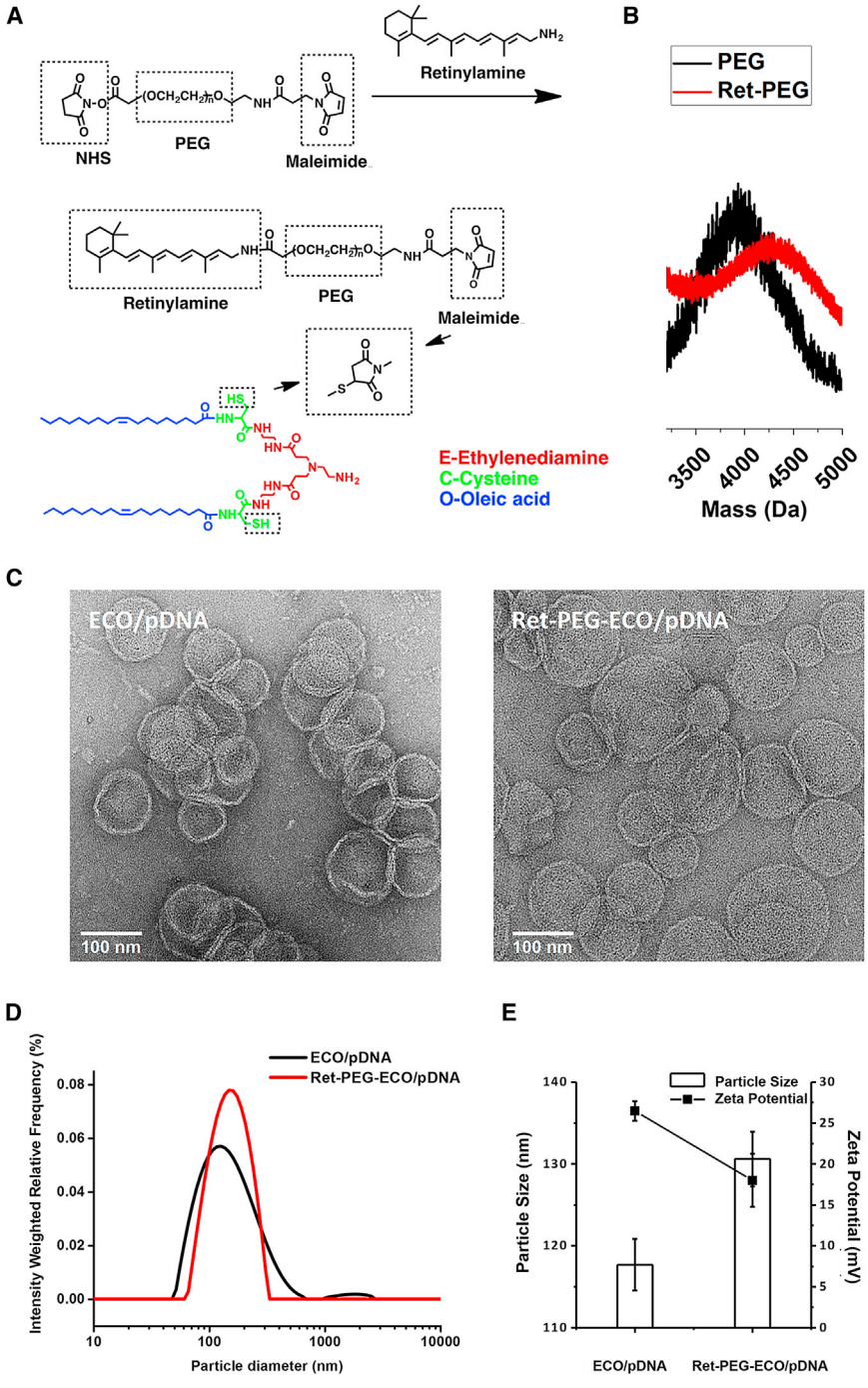

Figure 2. Preparation of the Targeting Ligand and Characterization of Ret-PEG-ECO/pDNA Nanoparticles

(A) Synthesis route. (B) MALDI-TOF mass spectrum of Ret-PEG-MAL. (C) TEM images of Ret-PEG-ECO/pDNA nanoparticles. (D) Size distribution of Ret-PEG-ECO/pDNA nanoparticles measured by DLS. (E) Sizes and zeta potentials of Ret-PEG-ECO/pDNA nanoparticles. Each bar represents the mean ± size of particles and each dot represents the mean ± zeta potential of particles (n = 3).

then formed by self-assembly with pDNA. Figure 2C shows the transmission electron microscopy (TEM) images of the untargeted and targeted ECO/pDNA nanoparticles. The average size of ECO/pDNA nanoparticles was approximately 100 nm based on TEM. The average size of Ret-PEG-ECO/pDNA nanoparticles was around 120 nm, a slight increase after surface modification with Ret-PEG. The result was consistent with that measured by dynamic light scattering (DLS). Slight aggregation of ECO/pDNA nanoparticles might result in wider size distribution than Ret-PEG-ECO/pDNA nanoparticles in the size distribution curve, as shown in Figure 2D. After conjugation with the targeting ligand, little aggregation was observed for the Ret-PEG-ECO/pDNA nanoparticles with a narrow distribution of the particle size. The sizes and zeta potentials of ECO/pDNA and Ret-PEG-ECO/pDNA nanoparticles are depicted in Figure 2E. The average size of the ECO/pDNA nanoparticles (117 nm) was slightly smaller than that of the Ret-PEG-ECO/pDNA nanoparticles (131 nm) based on DLS measurements. After targeting ligand conjugation, the average zeta potential of Ret-PEG-ECO/pDNA nanoparticles dropped from 26 mV to 18 mV, which not only reduced the cytotoxicity but also stabilized the delivery system.

In Vivo Transfection with Targeted Ret-PEG-ECO/pGFP Nanoparticles in Wild-Type BALB/c Mice

The Ret-PEG-ECO/pGFP nanoparticles were subretinally injected in BALB/c mice to determine in vivo gene delivery and expression efficiency with GFP as a reporter gene. Significant GFP expression was observed in RPE flat mounts with both unmodified ECO/pGFP nanoparticles and targeted Ret-PEG-ECO/pGFP nanoparticles 3 days post-injection. However, Ret-PEG-ECO/pGFP nanoparticles produced greater GFP expression than ECO/pGFP nanoparticles (Figure 3A). ZO-1 staining of tight junction proteins in RPE flat mounts further confirmed that the enhanced GFP expression emanated from RPE cells (Figure 3B).

Gene Replacement Therapy with Ret-PEG-ECO/pRPE65 Nanoparticles in Rpe65$^{-/-}$ Mice

Gene therapy with all-*trans*-retinylamine modified ECO nanoparticles was carried out in *Rpe65*$^{-/-}$ mice in which *Rpe65* was completely

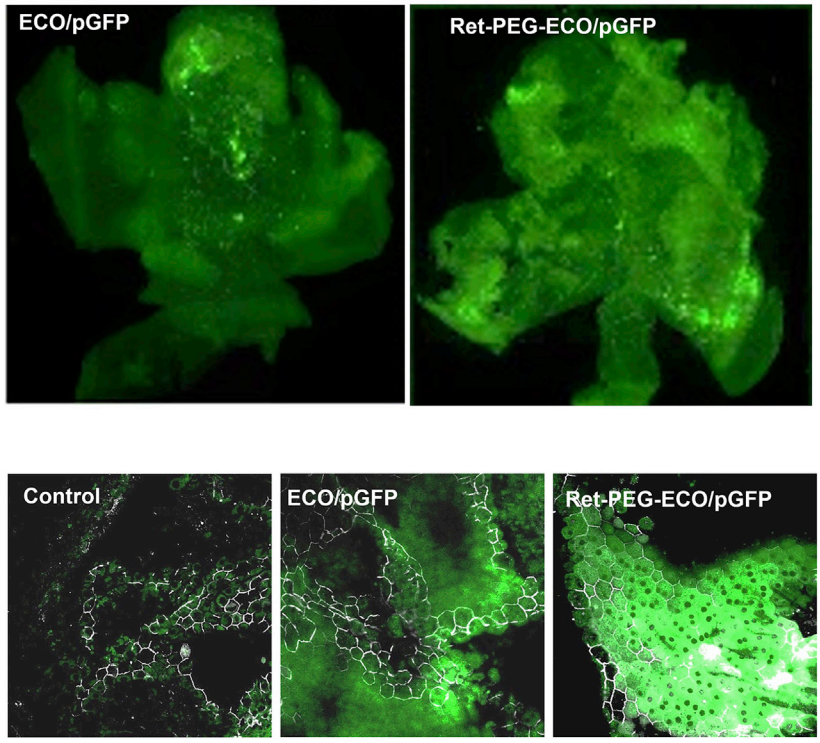

Figure 3. In Vivo Gene Transfection with Targeted Ret-PEG-ECO/pGFP Nanoparticles in Wild-Type BALB/c Mice

Mice (1 month old) were subretinally injected with ECO/pGFP or Ret-PEG-ECO/pGFP nanoparticles. RPE flat mounts were obtained 3 days post-transfection. (A) Fluorescence microscopic images showing enhanced GFP expression with Ret-PEG-ECO/pGFP nanoparticles in the RPE 3 days post-injection. (B) Confocal fluorescence microscopic images revealing GFP expression specifically in the RPE with anti-ZO-1 antibody staining (white). The tight junction protein ZO-1 represents the borders of the RPE cells.

knocked down. *Rpe65*$^{-/-}$ mice exhibit phenotypic features similar to human LCA2 patients.[34] Ret-PEG-ECO/pRPE65 nanoparticles were injected into the subretinal space of 1-month-old *Rpe65*$^{-/-}$ mice. 15 days post-injection, treatment with Ret-PEG-ECO/pRPE65 nanoparticles produced higher mRNA levels of RPE65 in the treated group than in the untreated control group (Figure 4A). This finding demonstrates successful introduction of the therapeutic gene. ERG was performed at an intensity of 1.6 log cd × s/m^2 to determine the efficacy of the nanoparticle treatment based on the electrical responses to light from the retina.[35] Figure 4B shows significant scotopic and photopic ERG response waveforms in the nanoparticle treatment group 7 days post-treatment, whereas there was almost no response in control group mice injected with Ret-PEG-ECO. The amplitudes of the major waves from all ERG tests were calculated 3, 7, 30, and 120 days post-treatment (Figures 4C–4F). Significant increases in the amplitudes of scotopic a-waves and b-waves were observed for nanoparticle-treated groups but not for control groups (vehicle-injected). Introduction of the exogenous *RPE65* gene increased about 50% of the scotopic ERG amplitude throughout all time points up to 120 days (Figures 4C and 4E), which demonstrated improved function of rod photoreceptors. Cone function also improved, represented by a 3- to 5-fold increase in photopic b-wave amplitude in the first 7 days after treatment. Although the amplitude decreased at later time points, the photopic b-wave amplitude of the treatment group was 2-fold that of the control, even at 120 days. Photopic a-waves were higher in the treatment groups than in the controls, but the difference was not statistically significant.

Cone Preservation after Gene Replacement Therapy with Ret-PEG-ECO/pRPE65 Nanoparticles in Rpe65$^{-/-}$ Mice

To determine whether Ret-PEG-ECO/pRPE65 nanoparticles could rescue cone cells in *Rpe65*$^{-/-}$ mice, we prepared cryo-sections of the whole retina at 120 days post-injection and stained cone cells with peanut agglutinin (green). Compared with the control group (Figure 5A), the treatment group (Figure 5B) revealed substantial green fluorescence staining, representing a greater number of healthy cone photoreceptors. This result also explains the increase in photopic wave amplitudes in the ERG. Interestingly, fewer cone cells were observed away from the injection site (Figure 5C), suggesting local rescue in this gene therapy approach.

Therapeutic Effect of Gene Replacement Therapy with Ret-PEG-ECO/pRPE65 Nanoparticles in 3-Month-Old Rpe65$^{-/-}$ Mice

To determine the optimal timing for gene replacement therapy of LCA2 with the targeted nanoparticles, we initiated *RPE65* gene therapy with Ret-PEG-ECO/pRPE65 nanoparticles in 3-month-old *Rpe65*$^{-/-}$ mice and performed ERG tests to evaluate its therapeutic efficacy. According to the ERG responses measured 7 and 30 days post-treatment, no differences were observed for scotopic and photopic waveforms between the treatment and control groups (Figure 6), indicating no observable improvement of retinal function. This result suggests that gene replacement therapy with targeted nanoparticles in these older mice was not as effective in restoring vision as in younger mice, likely because of the progression of irreversible retinal degeneration in older animals.

Safety Assessment of Ret-PEG-ECO/pRPE65 Nanoparticles in BALB/c Mice

To evaluate the safety of Ret-PEG-ECO/pRPE65 nanoparticles in gene therapy, the nanoparticles were injected into the subretinal space of healthy 1-month-old BALB/c mice, and ERG tests were carried out 7 and 30 days post-injection. ERG responses for both the nanoparticle-injected group and the un-injected group were comparable at each light intensity (Figure 7A). A slight decrease

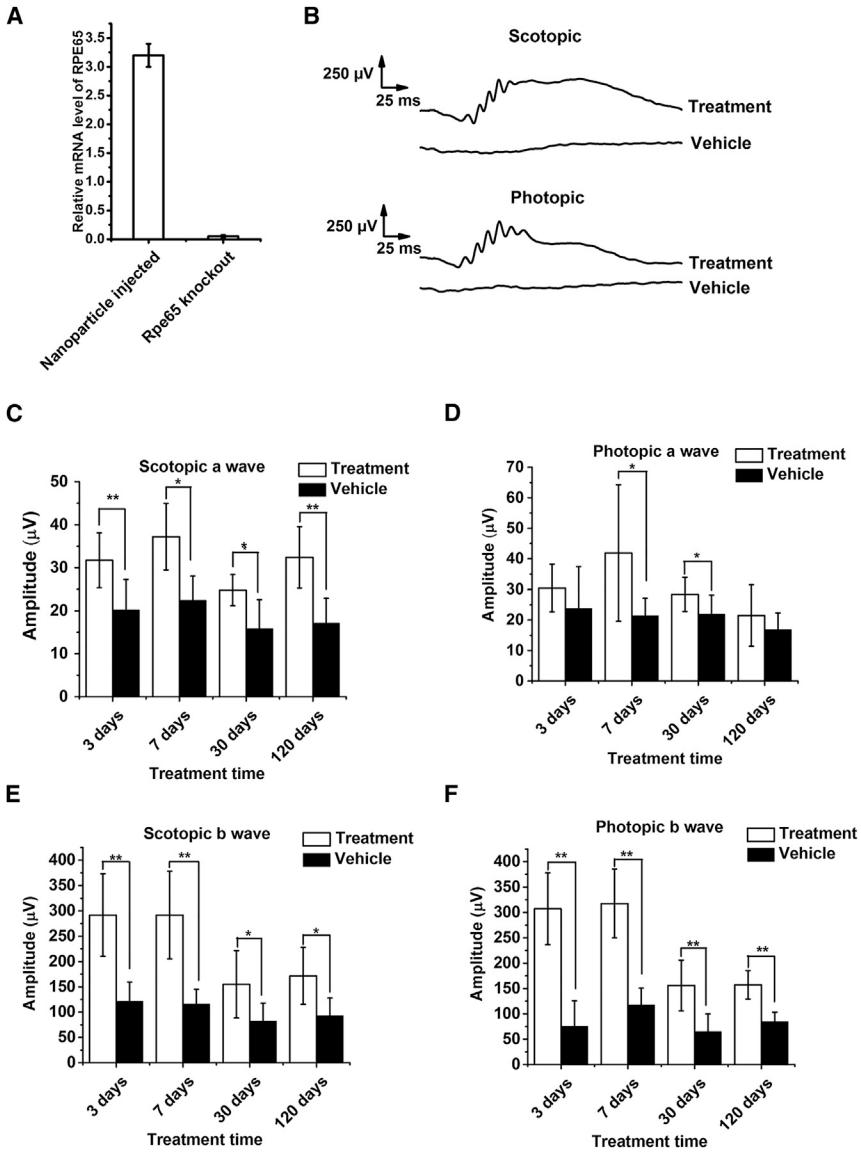

Figure 4. Gene Replacement Therapy with Ret-PEG-ECO/pRPE65 Nanoparticles in *Rpe65*$^{-/-}$ Mice

Mice were subretinally injected with Ret-PEG-ECO/pRPE65 nanoparticles or Ret-PEG-ECO. (A) Relative RPE65 mRNA levels in treated (pRPE65-injected) versus control groups 15 days after treatment. Each bar represents the mean ± mRNA expression level (n = 3). (B) Representative scotopic and photopic electroretinograms acquired from *Rpe65*$^{-/-}$ mice under the light intensity of 1.6 log cd × s/m^2 7 days after treatment. (C–F) Amplitudes of scotopic a-waves (C), photopic a-waves (D), scotopic b-waves (E), and photopic b-waves (F) of treated and control *Rpe65*$^{-/-}$ mice 3, 7, 30, and 120 days post-injection (**$p < 0.005$). Each bar represents the mean ± wave amplitude ($n \geq 3$).

in response amplitudes was observed for some major waveforms 7 days post-injection because of the induced inflammation. Eye function after nanoparticle injection became normal at 30 days, and no deleterious effects were noted in the ERG major wave amplitudes (Figures 7B–7E). This result indicates that Ret-PEG-ECO/pRPE65 nanoparticles are safe for subretinal injection in gene replacement therapy.

DISCUSSION

Gene replacement therapy holds great promise for treating monogenic vision disorders. Thus, establishing a gene delivery system with high transfection efficiency, good therapeutic efficacy, and a high safety profile is critical for broad clinical applications of this treatment. Gene therapy with AAV[1] has been extensively investigated for treatment of LCA2, a monogenic genetic disease. Although gene delivery by AAV has been reported as successful in LCA2,[8,9] its application is limited for treating other monogenic ocular diseases because some therapeutic genes are too large to be loaded into this viral vector. Design of a safe and efficient non-viral gene delivery system has the potential to circumvent this limitation in gene therapy of monogenic visual disorders.

ECO is a multifunctional lipid that has demonstrated excellent efficiency for cytosolic delivery of a variety of genetic materials because of its intrinsic PERC effect.[22–26] This study has shown that ECO is also effective for delivering therapeutic pDNA for non-viral gene replacement therapy in *Rpe65*$^{-/-}$ mice. The superior transfection properties of ECO/pDNA nanoparticles result from the multifunctional properties of the lipid carrier, including self-assembly formation of stable nanoparticles with pDNA without helper lipids, pH-sensitive amphiphilic cell membrane destabilization and endosomal escape, as well as reductive dissociation of the nanoparticles to release nucleic acids in the cytoplasm.[22,26] Here we tested a targeting mechanism that involves the use of IRBP to enhance pDNA delivery with ECO into RPE cells (Figure 8). In the retina, the interphotoreceptor matrix fills the space between rod outer segment and RPE cells, where IRBP is the major carrier that selectively transports all-*trans*-retinol from photoreceptor cells to RPE cells.[28] Modification of ECO/pDNA nanoparticles with this all-*trans*-retinoid can then facilitate their binding to IRBPs for enhanced delivery to the RPE. When injected into the subretinal space, IRBPs will quickly bind the targeting ligand and help to transport and release the particles near the apical side of the RPE before being internalized by the RPE cells.[33] In vivo transfection with pGFP demonstrated the enhanced gene transfer and expression efficiency of ECO/pDNA nanoparticles with this targeting mechanism in the RPE.

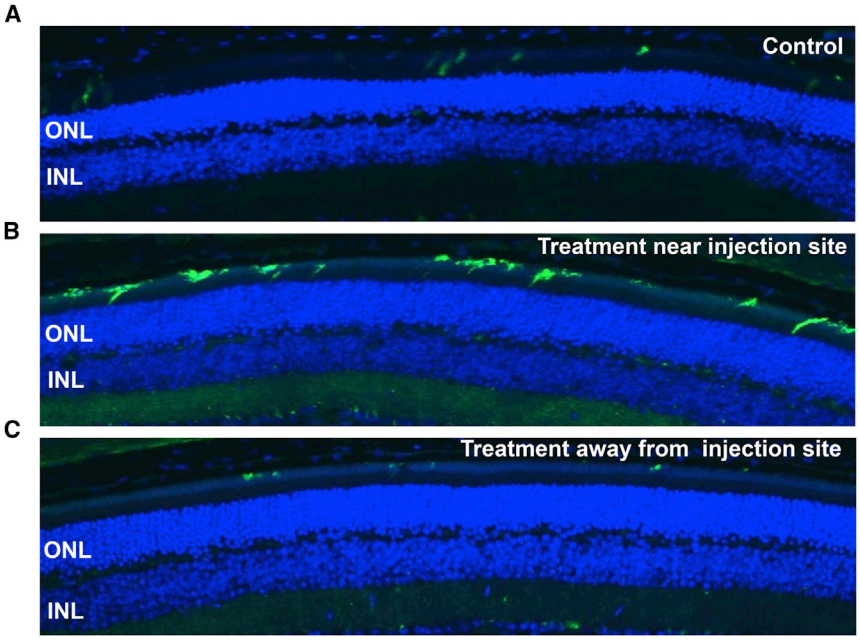

Figure 5. Cone Preservation after Gene Replacement Therapy with Ret-PEG-ECO/pRPE65 Nanoparticles in *Rpe65*$^{-/-}$ Mice 120 Days after Treatment

(A–C) Peanut agglutinin (green) was used to stain cone photoreceptors. Nuclei were stained with DAPI (blue).

Gene replacement therapy using Ret-PEG-ECO/pRPE65 nanoparticles successfully introduced the expression of exogenous therapeutic *RPE65* genes in the RPE layer. ERG results in treated *Rpe65*$^{-/-}$ mice demonstrated a significant increase in function of both rod and cone photoreceptors, with a therapeutic effect comparable to that of viral gene delivery systems.[36] In addition to protecting the RPE, Ret-PEG-ECO/pRPE65 treatment protected cone photoreceptors adjacent to the injection sites in these mice, slowing cone degeneration for at least 4 months. This therapeutic effect is similar to that reported for viral delivery of RPE65, which also delayed cone degeneration 4 months post-injection in *Rpe65*$^{-/-}$ mice.[37] Furthermore, gene therapy with Ret-PEG-ECO/pRPE65 nanoparticles has demonstrated a safe profile that does not irreversibly damage the retina. The slight drop in ERG major wave amplitudes caused by the injection's inflammatory effect recovered shortly after the injection.

Similar to the phenotype of human LCA2 patients, mice with *RPE65* gene knockout have diminished ERG responses because the supply of the 11-*cis*-retinal visual chromophore cannot be regenerated. Rather than producing the chromophore, the impaired visual cycle accumulates the intermediate product all-*trans*-retinyl ester in the RPE, which gradually damages the retina. Massive degeneration of cone cells can occur as early as 1 month of age in *Rpe65*$^{-/-}$ mice. Photoreceptor outer segment abnormalities are commonly visible at 1 or 2 months of age, and the outer nuclear layer is thinner than normal at 3 months of age.[34] After introduction of the exogenous *RPE65* gene to the RPE layer of 1-month-old mice, even in a small number of RPE cells, the visual cycle can supply sufficient 11-*cis*-retinal for the adjacent photoreceptor cell layer to provide improved visual function.[38]

Rescue of cone cells because of Ret-PEG-ECO/pRPE65 nanoparticle gene therapy could also be attributed to *RPE65* expression in such cells as well as in RPE cells. This effect was also reported in a clinical trial that demonstrated a cone rescue effect after gene therapy.[9] Although the treatment was effective in 1-month-old mice, treatment of 3-month-old mice with Ret-PEG-ECO/pRPE65 nanoparticles had no effect because the photoreceptor cells had begun to degenerate by this age. The observation is consistent with human patients with LCA2. During the first few years of life, children with LCA2 are less visually responsive than healthy children. Older LCA2 patients demonstrate more severe retinal degeneration that makes the retina less responsive to RPE65 gene therapy.

Other strategies have been reported previously to target the RPE layer. For example, hyaluronan has been applied to target CD44 receptors expressed by RPE cells. Folate has been tested as a targeting ligand for folate receptors associated with the RPE.[39,40] However, the expression of CD44 receptors is more restricted in inflammatory tissue, and folate receptors reside predominantly in the basal rather than apical membranes of RPE cells. Therefore, the distribution of these receptors greatly restricts the use of these ligands to target the RPE. By comparison, targeting IRBPs with the all-*trans*-retinyl group can avoid the restrictions of the targeting mechanisms reported above and provide efficient gene delivery to RPE cells after subretinal injection.

Here we have demonstrated the efficacy of a targeted gene delivery system for gene replacement in LCA2. However, improvements are needed to optimize the system prior to clinical translation. These include prolonging gene expression, identifying the appropriate disease stage for maximal effectiveness of therapy, and exploring alternate routes of injection to transfect the whole RPE layer. In future work, we will address the transience of gene expression with these nanoparticles by modifying the DNA plasmid with sequences that prolong gene expression, such as scaffold/matrix attachment regions (S/MARs).[41] The targeted ECO/pDNA nanoparticles can also be further optimized by introducing a pH-sensitive spacer between PEG and ECO to enhance endosomal escape of the ECO/pDNA nanoparticles.[42] Although modification of ECO/pDNA with Ret-PEG promoted cellular uptake of the nanoparticles, the PEG layer could hinder the pH-sensitive amphiphilic endosomal escape of the ECO/pDNA nanoparticles. Incorporation

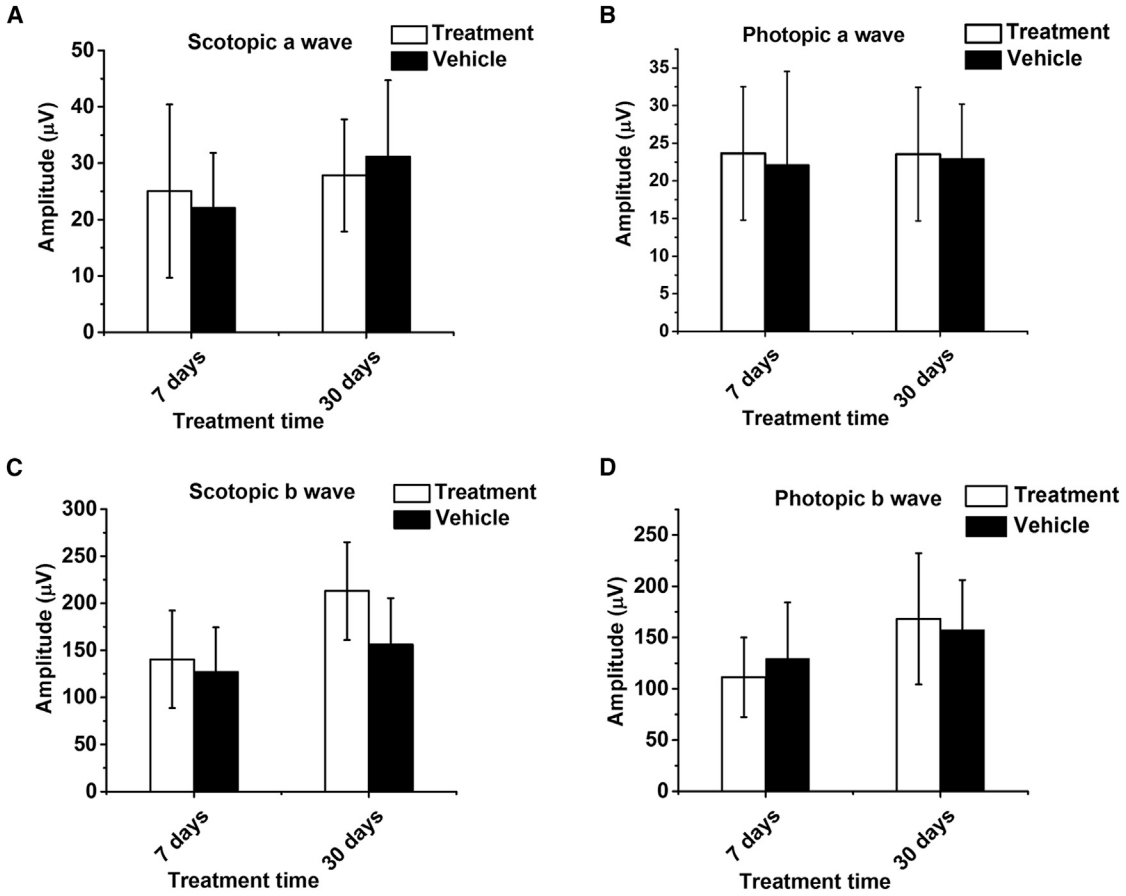

Figure 6. Therapeutic Effect of Gene Replacement Therapy with Ret-PEG-ECO/pRPE65 Nanoparticles in 3-Month-Old *Rpe65*$^{-/-}$ Mice

Shown are ERG amplitudes of major response waveforms. (A–D) Scotopic a-waves (A), photopic a-waves (B), scotopic b-waves (C), and photopic b-waves (D) in the treatment and control groups of *Rpe65*$^{-/-}$ mice. Each bar represents the mean ± wave amplitude ($n \geq 3$).

of a pH-sensitive hydrazone spacer will shed the PEG layer via pH-sensitive hydrolysis of hydrazone in acidic endosomes. This will expose the core ECO/pDNA nanoparticles to enhance endosomal escape, with cytosolic gene delivery and increased expression of the therapeutic gene.

In conclusion, the multifunctional lipid ECO-based gene delivery system used here demonstrated excellent gene transfection efficiency because of its unique ability to escape from the endosome. Modification of ECO/pDNA nanoparticles with all-*trans*-retinylamine to target RPE cells greatly enhanced transfection efficiency in the RPE in vivo. Gene replacement therapy with Ret-PEG-ECO/pRPE65 nanoparticles significantly improved the ERG activity and vision of *Rpe65*$^{-/-}$ mice, and this therapeutic effect continued for at least 120 days. Ret-PEG-ECO/pRPE65 nanoparticles were safe for subretinal injection, as shown in wild-type BALB/c mice. All-*trans*-retinylamine-modified pH-sensitive ECO/pDNA nanoparticles comprise a promising non-viral platform for safe, efficient, and targeted delivery of gene therapeutics to treat RPE tissue-specific monogenic eye diseases, including LCA2.

MATERIALS AND METHODS

Cell Cultures

ARPE-19 cells were cultured in DMEM and supplemented with 10% fetal bovine serum, 100 μg/mL streptomycin, and 100 units/mL penicillin (all reagents were from Invitrogen). Cells were maintained in a humidified incubator at 37°C and 5% CO_2.

Animals

BALB/c wild-type mice were purchased from Jackson Laboratory. *Rpe65*$^{-/-}$-deficient C57BL6 mice were obtained from Michael Redmond (National Eye Institute, NIH) and genotyped as described previously.[43] All mice were housed and cared for in the animal facility at the School of Medicine, Case Western Reserve University, and all animal procedures were approved by the Case Western Reserve University (CWRU) Institutional Animal Care and Use Committee.

Synthesis of Ret-PEG-MAL

All-*trans*-retinylamine (15 mg) and MAL-PEG-succinimidyl carboxymethyl (SCM) (molecular weight [MW] = 3,400 Da, NANOCS) (55 mg) were added to 15 mL dimethylformamide. The solution was

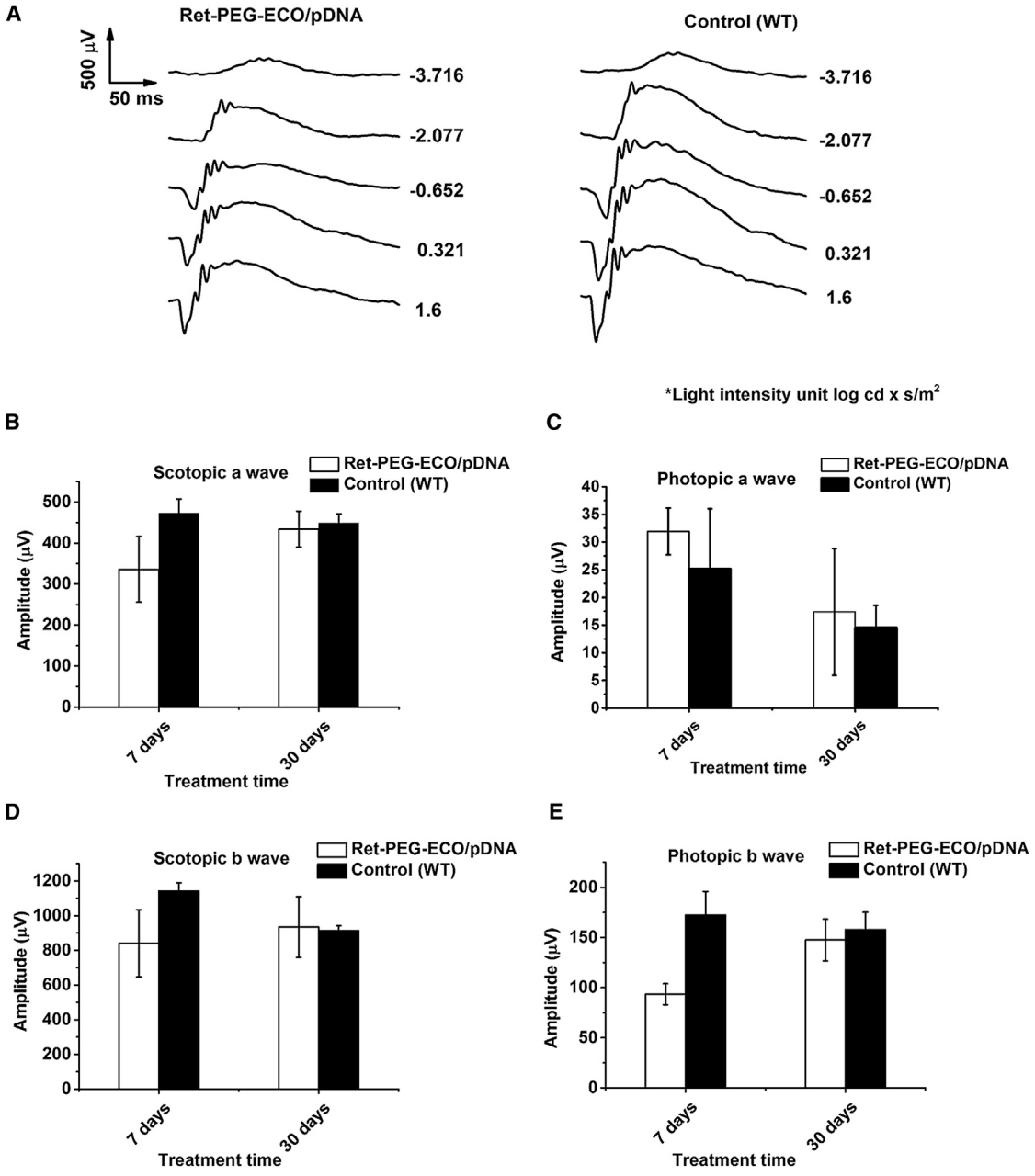

Figure 7. Safety Assessment of Ret-PEG-ECO/pRPE65 Nanoparticles in 1-Month-Old BALB/c Mice

(A) Representative ERG traces of scotopic waveforms in the PEG-ECO/pRPE65-treated group and untreated mice 30 days post-injection. (B–E) ERG amplitudes of scotopic a-waves (B), photopic a-waves (C), scotopic b-waves (D), and photopic b-waves (E) in treated and control animals. Each bar represents the mean ± wave amplitude ($n \geq 3$).

stirred at room temperature overnight. The product Ret-PEG-MAL was precipitated in 50 mL diethyl ether and washed three times. The product was dried under vacuum to give Ret-PEG-MAL (yield, 89%).

Preparation of ECO/pDNA and Ret-PEG-ECO/pDNA Nanoparticles

Multifunctional pH-sensitive lipid ECO was synthesized as reported previously.[24] The ECO/pDNA nanoparticles were prepared by self-assembly of ECO with plasmid DNA at an amine/phosphate (N/P) ratio of 6. The ECO stock solution (2.5 mM in ethanol) and plasmid DNA stock solution (0.5 mg/mL) at predetermined amounts based on the N/P ratio were diluted into equal volumes with nuclease-free water, mixed, and shaken for 30 min at room temperature. The Ret-PEG-MAL solution (0.4 mM in 50% DMSO and water) was then added to the mixture at 2.5 mol % and shaken for another 30 min to facilitate the reaction between the maleimide functional

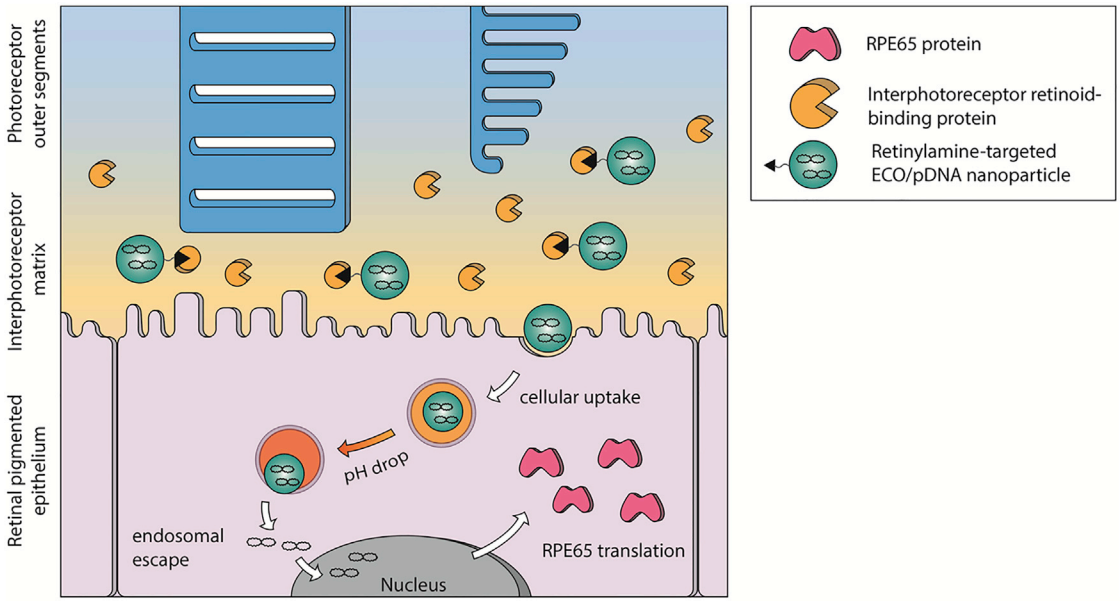

Figure 8. Targeting Mechanism of All-*trans*-Retinylamine-Modified ECO Nanoparticles

When injected into the subretinal space, all-*trans*-retinylamine-modified ECO nanoparticles will bind to IRBP in the interphotoreceptor matrix. IRBP binding helps to retain the nanoparticles in the space and transports the nanoparticles to the target cells in the RPE. Following cellular uptake by endocytosis, the nanoparticles escape from the endosomal compartment and release the RPE65 plasmid DNA via the PERC mechanism. Finally, the RPE65 gene is expressed by the RPE cell, where it slows cone cell degeneration and preserves visual function.

group and free thiols on ECO. A different ECO stock solution (25 mM) was used for in vivo formulations. Lipofectamine 2000 (Invitrogen)/DNA nanoparticles were prepared according to the manufacturer's recommendations.

TEM

The morphology of ECO/pDNA (N/P = 6) and Ret-PEG-ECO/pDNA (N/P = 6) nanoparticles was imaged with a transmission electron microscope (JEOL JEM2200FS). Samples for TEM were prepared by depositing 20 μL of the particle solution onto a 300-mesh copper grid covered by a thin amorphous carbon film (20 nm). Immediately after deposition, the excess liquid was removed by touching the grid with filter paper. Samples were stained twice by adding 3 μL 2% uranyl acetate aqueous solution; the excess of staining solution was removed after each addition. Images of the nanoparticles were acquired by TEM after the samples were dried.

DLS

The sizes and zeta potentials of ECO/pDNA (N/P = 6) and Ret-PEG-ECO/pDNA (N/P = 6) nanoparticles were determined by DLS with an Anton Paar Litesizer 500 (Anton Paar USA). Three measurements were performed and averaged for each sample at 20°C.

In Vitro Transfection

ARPE-19 cells were seeded onto 12-well plates at a density of 4×10^4 cells/well and allowed to grow for 24 hr at 37°C. Transfections were conducted in 10% fetal bovine serum medium with the ECO nanoparticles of GFP plasmid DNA (Altogen Biosystems) at a DNA concentration of 1 μg/mL. ECO/pGFP nanoparticles were incubated with ARPE-19 cells for 8 hr at 37°C. The medium was then replaced with fresh serum-containing medium (10% serum), and cells were then cultured for an additional 48 hr. GFP expression was evaluated with an Olympus FV1000 confocal microscope (Olympus). After removal of the culture medium, each well was washed twice with PBS (10 mM sodium phosphate [pH 7.2] and 100 mM NaCl). Cells were harvested after treatment with 0.25% trypsin containing 0.26 mM EDTA (Invitrogen), followed by centrifugation at 1,000 rpm for 5 min and fixation in 750 μL PBS containing 4% paraformaldehyde, and finally passed through a 35-μm cell strainer (BD Biosciences). A BD FACSCalibur flow cytometer (BD Biosciences) was used to determine GFP expression based on the fluorescence intensity from a total of 10,000 cells for each sample.

Intracellular Uptake

ARPE-19 cells (4×10^4/well) were seeded onto glass-bottom microwell dishes and allowed to grow for 24 hr at 37°C before they were stained with 4 μg/mL Hoechst 33342 (Invitrogen) and 100 mM LysoTracker Green (Life Technologies). Cells then were treated with ECO/Cy3-pDNA (Mirus Bio, catalog number MIR7904, N/P = 6) nanoparticles in 10% fetal bovine serum medium. Cells were cultured with nanoparticles for 1, 4, and 24 hr (media were replaced by fresh media after 4 hr), and then the media were removed, and cells were washed with PBS three times before fixation with PBS containing 4% paraformaldehyde. Fluorescence images were acquired with an Olympus FV1000 confocal microscope.

In Vivo Subretinal Transfection with ECO/pDNA and Ret-PEG-ECO/pDNA Nanoparticles

All surgical manipulations were carried out under a surgical microscope (Leica M651 MSD). Mice were anesthetized by intraperitoneal injection of a cocktail (15 μL/g body weight) comprised of ketamine (6 mg/mL) and xylazine (0.44 mg/mL) in PBS buffer (10 mM sodium phosphate and 100 mM NaCl [pH 7.2]). Pupils were dilated with 1.0% tropicamide ophthalmic solution (Bausch & Lomb). A 33G beveled needle (World Precision Instruments) was used as a lance to make a full-thickness cut through the sclera 1.0 mm posterior to the limbus. This needle then was replaced with a 36G beveled needle attached to an injection system (UMP-II microsyringe pump and a Micro4 controller with a footswitch, World Precision Instruments). The needle was aimed toward the inferior nasal area of the retina, and an ECO/pDNA or Ret-PEG-ECO/pDNA nanoparticles solution (2.4 μL) was injected to deliver either a pRPE65 (OriGene) or pGFP at the dose of 240 ng into the subretinal space. Successful administration was confirmed by bleb formation. The tip of the needle remained in the bleb for 10 s after bleb formation, when it was gently withdrawn. A solution (2.4 μL) of Ret-PEG-ECO carrier alone with the same concentration as Ret-PEG-ECO/pDNA nanoparticles was also injected into the subretinal space of the contra eye to serve as a control. Each of the group included at least three eyes with successful subretinal injection. To assess GFP expression, the mice were sacrificed, and eyes were collected 3 days after injection, washed with penicillin-streptomycin solution (Sigma), and rinsed with Hank's balanced salt solution (HyClone). Eye cups were prepared as described previously.[26] The retina and RPE layers were placed in glass-bottom confocal plates and fixed with 1 mL of PBS containing 4% paraformaldehyde. GFP expression in the RPE layer was evaluated with an Olympus FV1000 confocal microscope.

qRT-PCR

Rpe65$^{-/-}$ mice were sacrificed 15 days after subretinal injection with Ret-PEG-ECO/pRPE65 nanoparticles, and RNA was isolated from their eyes. cDNA was synthesized with the QuantiTect reverse transcription kit (QIAGEN) following the manufacturer's instructions. qRT-PCR amplification was performed with SYBR Green I Master mix (Roche Diagnostics). Fold changes were calculated after normalizing the data to glyceraldehyde 3-phosphate dehydrogenase. *Rpe65*$^{-/-}$ mice without treatment were used as controls.

Electroretinograms

Electroretinograms were acquired according to a reported method.[44] Animals were anesthetized by intraperitoneal injection of a cocktail (15 μL/g body weight) comprised of ketamine (6 mg/mL) and xylazine (0.44 mg/mL) in PBS buffer (10 mM sodium phosphate and 100 mM NaCl [pH 7.2]). Pupils were dilated with 1% tropicamide for imaging. Experiments were performed in a dark room. Three electrodes were placed on each mouse: a contact lens electrode on the eye, a reference electrode underneath the skin between the ears, and a ground electrode underneath the skin of the tail. Electroretinograms were recorded with the universal electrophysiologic system UTAS E-3000 (LKC Technologies).

Histology

Eye cups were fixed in 2% glutaraldehyde and 4% paraformaldehyde and processed with optimum cutting temperature (OCT) formulation. Sections were cut at 1 μm. The sample slides were permeabilized and fixed sequentially with 4% paraformaldehyde (PFA) and 0.25% Triton X-100, followed by treatment with 0.5% BSA blocking solution for 1 hr at room temperature. The fluorescence labeled peanut agglutinin (PNA) was applied at a concentration of 12.5 μg/mL for 1 hr at room temperature and washed three times with a 0.1% Tris-buffered saline with Tween 20 (TBST) solution for 5 min each time. Slides were counter-stained with DAPI and mounted with a coverslip using the Prolong Gold reagent (Invitrogen) before imaging. Stained tissue was imaged with an Olympus FV1000 confocal microscope.

Statistical Analysis

Statistical analyses were conducted with two-tailed Student's t tests using a 95% confidence interval. Statistical significance was accepted when $p \leq 0.05$.

AUTHOR CONTRIBUTIONS

Z.R.L. conceived the project. D.S. was involved in all aspects of this work. B.S. performed subretinal injections and tissue sample analysis. S.G. performed ERG examinations. R.M.S. performed data analysis. A.M. and K.P. provided assistance with animal model and equipment design. D.S., S.G., R.M.S., A.M.V., A.M., K.P., and Z.R.L. contributed to the study design and manuscript preparation. All authors read and approved the final paper.

CONFLICTS OF INTEREST

Z.R.L. is one of the founders of Cleveland Theranostics LLC. D.S. and Z.R.L. have ownership interest in a patent application.

ACKNOWLEDGMENTS

Z.R.L. is an M. Frank Rudy and Margaret Domiter Rudy Professor of Biomedical Engineering, and K.P. is a John H. Hord Professor of Pharmacology. The DLS experiment was finished with the help of Ms. Nadia R. Ayat.

REFERENCES

1. Hufnagel, R.B., Ahmed, Z.M., Corrêa, Z.M., and Sisk, R.A. (2012). Gene therapy for Leber congenital amaurosis: advances and future directions. Graefes Arch. Clin. Exp. Ophthalmol. *250*, 1117–1128.

2. Koenekoop, R.K. (2004). An overview of Leber congenital amaurosis: a model to understand human retinal development. Surv. Ophthalmol. *49*, 379–398.

3. Stone, E.M. (2007). Leber congenital amaurosis - a model for efficient genetic testing of heterogeneous disorders: LXIV Edward Jackson Memorial Lecture. Am. J. Ophthalmol. *144*, 791–811.

4. Golczak, M., Kiser, P.D., Lodowski, D.T., Maeda, A., and Palczewski, K. (2010). Importance of membrane structural integrity for RPE65 retinoid isomerization activity. J. Biol. Chem. *285*, 9667–9682.

5. Kiser, P.D., Zhang, J., Badiee, M., Li, Q., Shi, W., Sui, X., Golczak, M., Tochtrop, G.P., and Palczewski, K. (2015). Catalytic mechanism of a retinoid isomerase essential for vertebrate vision. Nat. Chem. Biol. *11*, 409–415.

6. Kiser, P.D., and Palczewski, K. (2010). Membrane-binding and enzymatic properties of RPE65. Prog. Retin. Eye Res. *29*, 428–442.

7. Aguirre, G.D., Baldwin, V., Pearce-Kelling, S., Narfström, K., Ray, K., and Acland, G.M. (1998). Congenital stationary night blindness in the dog: common mutation in the RPE65 gene indicates founder effect. Mol. Vis. *4*, 23.
8. Simonelli, F., Maguire, A.M., Testa, F., Pierce, E.A., Mingozzi, F., Bennicelli, J.L., Rossi, S., Marshall, K., Banfi, S., Surace, E.M., et al. (2010). Gene therapy for Leber's congenital amaurosis is safe and effective through 1.5 years after vector administration. Mol. Ther. *18*, 643–650.
9. Jacobson, S.G., Cideciyan, A.V., Ratnakaram, R., Heon, E., Schwartz, S.B., Roman, A.J., Peden, M.C., Aleman, T.S., Boye, S.L., Sumaroka, A., et al. (2012). Gene therapy for leber congenital amaurosis caused by RPE65 mutations: safety and efficacy in 15 children and adults followed up to 3 years. Arch. Ophthalmol. *130*, 9–24.
10. Mueller, C., and Flotte, T.R. (2008). Clinical gene therapy using recombinant adeno-associated virus vectors. Gene Ther. *15*, 858–863.
11. Ginn, S.L., Alexander, I.E., Edelstein, M.L., Abedi, M.R., and Wixon, J. (2013). Gene therapy clinical trials worldwide to 2012 - an update. J. Gene Med. *15*, 65–77.
12. Cideciyan, A.V., Hauswirth, W.W., Aleman, T.S., Kaushal, S., Schwartz, S.B., Boye, S.L., Windsor, E.A., Conlon, T.J., Sumaroka, A., Pang, J.J., et al. (2009). Human RPE65 gene therapy for Leber congenital amaurosis: persistence of early visual improvements and safety at 1 year. Hum. Gene Ther. *20*, 999–1004.
13. Hauswirth, W.W., Aleman, T.S., Kaushal, S., Cideciyan, A.V., Schwartz, S.B., Wang, L., Conlon, T.J., Boye, S.L., Flotte, T.R., Byrne, B.J., and Jacobson, S.G. (2008). Treatment of leber congenital amaurosis due to RPE65 mutations by ocular subretinal injection of adeno-associated virus gene vector: short-term results of a phase I trial. Hum. Gene Ther. *19*, 979–990.
14. Jooss, K., and Chirmule, N. (2003). Immunity to adenovirus and adeno-associated viral vectors: implications for gene therapy. Gene Ther. *10*, 955–963.
15. Provost, N., Le Meur, G., Weber, M., Mendes-Madeira, A., Podevin, G., Cherel, Y., Colle, M.A., Deschamps, J.Y., Moullier, P., and Rolling, F. (2005). Biodistribution of rAAV vectors following intraocular administration: evidence for the presence and persistence of vector DNA in the optic nerve and in the brain. Mol. Ther. *11*, 275–283.
16. Wasungu, L., and Hoekstra, D. (2006). Cationic lipids, lipoplexes and intracellular delivery of genes. J. Control. Release *116*, 255–264.
17. Martin, B., Sainlos, M., Aissaoui, A., Oudrhiri, N., Hauchecorne, M., Vigneron, J.-P., Lehn, J.M., and Lehn, P. (2005). The design of cationic lipids for gene delivery. Curr. Pharm. Des. *11*, 375–394.
18. Shcharbin, D.G., Klajnert, B., and Bryszewska, M. (2009). Dendrimers in gene transfection. Biochemistry (Mosc.) *74*, 1070–1079.
19. Godbey, W.T., Wu, K.K., and Mikos, A.G. (1999). Poly(ethylenimine) and its role in gene delivery. J. Control. Release *60*, 149–160.
20. de la Fuente, M., Raviña, M., Paolicelli, P., Sanchez, A., Seijo, B., and Alonso, M.J. (2010). Chitosan-based nanostructures: a delivery platform for ocular therapeutics. Adv. Drug Deliv. Rev. *62*, 100–117.
21. Glover, D.J., Lipps, H.J., and Jans, D.A. (2005). Towards safe, non-viral therapeutic gene expression in humans. Nat. Rev. Genet. *6*, 299–310.
22. Wang, X.-L., Ramusovic, S., Nguyen, T., and Lu, Z.-R. (2007). Novel polymerizable surfactants with pH-sensitive amphiphilicity and cell membrane disruption for efficient siRNA delivery. Bioconjug. Chem. *18*, 2169–2177.
23. Gujrati, M., Malamas, A., Shin, T., Jin, E., Sun, Y., and Lu, Z.R. (2014). Multifunctional cationic lipid-based nanoparticles facilitate endosomal escape and reduction-triggered cytosolic siRNA release. Mol. Pharm. *11*, 2734–2744.
24. Malamas, A.S., Gujrati, M., Kummitha, C.M., Xu, R., and Lu, Z.R. (2013). Design and evaluation of new pH-sensitive amphiphilic cationic lipids for siRNA delivery. J. Control. Release *171*, 296–307.
25. Parvani, J.G., Gujrati, M.D., Mack, M.A., Schiemann, W.P., and Lu, Z.R. (2015). Silencing β3 integrin by targeted ECO/siRNA nanoparticles inhibits EMT and metastasis of triple-negative breast cancer. Cancer Res. *75*, 2316–2325.
26. Sun, D., Maeno, H., Gujrati, M., Schur, R., Maeda, A., Maeda, T., Palczewski, K., and Lu, Z.R. (2015). Self-assembly of a multifunctional lipid with core-shell dendrimer DNA nanoparticles enhanced efficient gene delivery at low charge ratios into RPE cells. Macromol. Biosci. *15*, 1663–1672.
27. D'Ambrosio, D.N., Clugston, R.D., and Blaner, W.S. (2011). Vitamin A metabolism: an update. Nutrients *3*, 63–103.
28. Gonzalez-Fernandez, F., and Ghosh, D. (2008). Focus on Molecules: interphotoreceptor retinoid-binding protein (IRBP). Exp. Eye Res. *86*, 169–170.
29. Vachali, P.P., Besch, B.M., Gonzalez-Fernandez, F., and Bernstein, P.S. (2013). Carotenoids as possible interphotoreceptor retinoid-binding protein (IRBP) ligands: a surface plasmon resonance (SPR) based study. Arch. Biochem. Biophys. *539*, 181–186.
30. Gonzalez-Fernandez, F. (2003). Interphotoreceptor retinoid-binding protein–an old gene for new eyes. Vision Res. *43*, 3021–3036.
31. Jin, M., Li, S., Nusinowitz, S., Lloyd, M., Hu, J., Radu, R.A., Bok, D., and Travis, G.H. (2009). The role of interphotoreceptor retinoid-binding protein on the translocation of visual retinoids and function of cone photoreceptors. J. Neurosci. *29*, 1486–1495.
32. Gonzalez-Fernandez, F. (2002). Evolution of the visual cycle: the role of retinoid-binding proteins. J. Endocrinol. *175*, 75–88.
33. Chen, Y., Houghton, L.A., Brenna, J.T., and Noy, N. (1996). Docosahexaenoic acid modulates the interactions of the interphotoreceptor retinoid-binding protein with 11-cis-retinal. J. Biol. Chem. *271*, 20507–20515.
34. Cideciyan, A.V. (2010). Leber congenital amaurosis due to RPE65 mutations and its treatment with gene therapy. Prog. Retin. Eye Res. *29*, 398–427.
35. Gresh, J., Goletz, P.W., Crouch, R.K., and Rohrer, B. (2003). Structure-function analysis of rods and cones in juvenile, adult, and aged C57bl/6 and Balb/c mice. Vis. Neurosci. *20*, 211–220.
36. Lai, C.-M., Yu, M.J., Brankov, M., Barnett, N.L., Zhou, X., Redmond, T.M., Narfstrom, K., and Rakoczy, P.E. (2004). Recombinant adeno-associated virus type 2-mediated gene delivery into the Rpe65-/- knockout mouse eye results in limited rescue. Genet. Vaccines Ther. *2*, 3.
37. Bemelmans, A.-P., Kostic, C., Crippa, S.V., Hauswirth, W.W., Lem, J., Munier, F.L., Seeliger, M.W., Wenzel, A., and Arsenijevic, Y. (2006). Lentiviral gene transfer of RPE65 rescues survival and function of cones in a mouse model of Leber congenital amaurosis. PLoS Med. *3*, e347.
38. Smith, J., Ward, D., Michaelides, M., Moore, A.T., and Simpson, S. (2015). New and emerging technologies for the treatment of inherited retinal diseases: a horizon scanning review. Eye (Lond.) *29*, 1131–1140.
39. Gan, L., Wang, J., Zhao, Y., Chen, D., Zhu, C., Liu, J., and Gan, Y. (2013). Hyaluronan-modified core-shell liponanoparticles targeting CD44-positive retinal pigment epithelium cells via intravitreal injection. Biomaterials *34*, 5978–5987.
40. Suen, W.-L.L., and Chau, Y. (2013). Specific uptake of folate-decorated triamcinolone-encapsulating nanoparticles by retinal pigment epithelium cells enhances and prolongs antiangiogenic activity. J. Control. Release *167*, 21–28.
41. Koirala, A., Makkia, R.S., Conley, S.M., Cooper, M.J., and Naash, M.I. (2013). S/MAR-containing DNA nanoparticles promote persistent RPE gene expression and improvement in RPE65-associated LCA. Hum. Mol. Genet. *22*, 1632–1642.
42. Gujrati, M., Vaidya, A.M., Mack, M., Snyder, D., Malamas, A., and Lu, Z.R. (2016). Targeted Dual pH-Sensitive Lipid ECO/siRNA Self-Assembly Nanoparticles Facilitate In Vivo Cytosolic sieIF4E Delivery and Overcome Paclitaxel Resistance in Breast Cancer Therapy. Adv. Healthc. Mater. *5*, 2882–2895.
43. Redmond, T.M., Yu, S., Lee, E., Bok, D., Hamasaki, D., Chen, N., Goletz, P., Ma, J.X., Crouch, R.K., and Pfeifer, K. (1998). Rpe65 is necessary for production of 11-cis-vitamin A in the retinal visual cycle. Nat. Genet. *20*, 344–351.
44. Schur, R.M., Sheng, L., Sahu, B., Yu, G., Gao, S., Yu, X., Maeda, A., Palczewski, K., and Lu, Z.R. (2015). Manganese-enhanced MRI for preclinical evaluation of retinal degeneration treatments. Invest. Ophthalmol. Vis. Sci. *56*, 4936–4942.